Voltage-Enhancement Mechanisms of an Organic Dye in High Open-Circuit Voltage Solid-State Dye-Sensitized Solar Cells

Song-Rim Jang,[†,‡,∥] Kai Zhu,[†,∥] Min Jae Ko,[‡] Kyungkon Kim,[‡] Chulhee Kim,[§] Nam-Gyu Park,[‡,⊥,*] and Arthur J. Frank[†,*]

[†]Chemical and Materials Science Center, National Renewable Energy Laboratory (NREL), Golden, Colorado 80401, United States, [‡]Solar Cell Research Center, Materials Science and Technology Division, Korea Institute of Science and Technology (KIST), Seoul 136-791, Korea, [§]Department of Polymer Science and Engineering, Inha University, Incheon 402-751, Korea, and [⊥]School of Chemical Engineering and Department of Energy Science, Sungkyunkwan University, Suwon 440-746, Korea. [∥]These authors contributed equally to this work.

ABSTRACT Sensitization of solid-state dye-sensitized solar cells (SSDSSCs) with a new, organic donor-π-acceptor dye with a large molar absorption coefficient led to an open-circuit voltage of over 1 V at AM1.5 solar irradiance (100 mW/cm^2). Recombination of electrons in the TiO_2 film with the oxidized species in the hole-transfer material (HTM) was significantly slower with the organic dye than with a standard ruthenium complex dye. Density functional theory indicated that steric shielding of the electrons in the TiO_2 by the organic dye was important in reducing recombination. Preventing the loss of photoelectrons resulted in a significant voltage gain. There was no evidence that the organic dye contributed to the high voltage by shifting the band edges to more negative electrode potentials. Compared with an iodide-based liquid electrolyte, however, the more positive redox potential of the solid-state HTM used in the SSDSSCs favored higher voltages.

KEYWORDS: high V_{oc} · solid-state dye-sensitized solar cells · spiro-MeOTAD · organic sensitizer · recombination kinetics

Mesoscopic dye-sensitized solar cells (DSSCs) have received much attention as inexpensive and remarkably efficient solar devices.[1] The most extensively studied DSSCs consist of a monolayer of a ruthenium bipyridyl dye adsorbed to the surface of a thin nanocrystalline TiO_2 film supported on a transparent conducting oxide (TCO) glass substrate. The TiO_2 crystallites of the film are in contact with a liquid redox electrolyte containing iodide and triiodide ions that serve as a redox relay. The Ru complex is typically attached to the oxide surface *via* carboxyl pendant groups on the bipyridyl ligand. Photocurrent is generated when visible or near-infrared light absorption by the sensitizer leads to electron injection into the conduction band of TiO_2. Sunlight-to-electrical conversion efficiencies of over 11% at full sunlight (AM1.5 solar irradiance) have been reported for DSSCs incorporating Ru complexes for photon harvesting.[2,3] Recently, metal-free organic dyes have attracted attention owing to their potential for having higher absorption coefficients, synthetically more tunable spectral response, larger abundance and diversity of candidates, and lower cost than ruthenium-containing dyes. Dye-sensitized solar cells containing organic dyes and iodide (I_3^-/I^-)-based electrolytes are reported[4−7] to reach efficiencies of over 9%, approaching the efficiencies of the traditional DSSCs with Ru dyes and the same iodide-based liquid electrolyte.

In the past decade, there has been much effort to develop solid-state dye-sensitized solar cells (SSDSSCs) in which a solid-state hole-transporting material (HTM) replaces the iodide-containing electrolyte for dye regeneration and for hole transport to the counter electrode. One of the more interesting solid-state HTMs for this purpose is 2,2′,7,7′-tetrakis-(*N*,*N*-di-*p*-methoxyphenylamine)-9,9′-spirobifluorene (spiro-MeOTAD).[8−11] In principle, the spiro-MeOTAD-based SSDSSCs favor higher open-circuit voltages (V_{oc}) than the traditional DSSCs because the redox potential of spiro-MeOTAD is a better match for the Ru dye than that of the iodide electrolyte. However, because of the difficulty in completely filling the pores of the TiO_2 films with spiro-MeOTAD[12] and the relatively fast recombination kinetics,[13] SSDSSCs are limited to thinner dye-covered films[14,15] that often lead to poor light-harvesting properties.[16] To achieve high SSDSSC performance with the thinner TiO_2 films, dyes with high absorption coefficient are a necessity. In one case, V_{oc}

* Address correspondence to npark@skku.edu, arthur.frank@nrel.gov.

Received for review August 3, 2011 and accepted September 13, 2011.

Published online September 20, 2011
10.1021/nn2029567

above 1 V was obtained.[17] Besides light harvesting, the dye can, in principle, influence cell performance by altering the surface recombination kinetics and band-edge energetics of the TiO_2 film. A recent study[17] showed that an organic dye in a SSDSSC can induce band-edge movement resulting in higher voltages. Ruthenium complexes with hydrophobic moieties can improve V_{oc} by shielding photoelectrons in the TiO_2 nanocrystalline films from recombining with oxidized iodide species in the liquid electrolyte.[18,19] Whether organic dyes can also improve the voltage by retarding recombination has not been established. Information is also sparse on the specific interactions that occur between organic dyes and hole-conducting media and the resulting synergistic effects on the properties of solid-state and liquid electrolyte-based DSSCs. In the case of the solid-state DSSC, the effectiveness of a given sensitizer could depend strongly on the hole-conducting medium.

In this paper, the sensitizing properties of a newly developed organic sensitizer containing a π-conjugated oligophenylenevinylene bridge with an electron donor−acceptor moiety (TA-St-CA) were compared with those of the standard ruthenium Z907 dye in DSSCs containing either spiro-MeOTAD or the iodide electrolyte. The SSDSSC with the organic dye and spiro-MeOTAD is found to produce a V_{oc} of over 1 V under simulated solar irradiance (100 mW/cm^2). The voltage-enhancement mechanisms of the sensitizers and hole-conducting phases were characterized. The effects of light harvesting, band-edge movement, and recombination on the voltage were investigated. The sensitizing properties of the TA-St-CA dye compares favorably to those of the Z907 dye in SSDSSCs. Besides having a high molar absorption coefficient, the TA-St-CA dye is shown to retard recombination at the TiO_2/spiro-MeOTAD interface of the SSDSSC, leading to a substantial gain in V_{oc}.

RESULTS AND DISCUSSION

The structures of the organic D-π-A sensitizer TA-St-CA, Z907 sensitizer, and spiro-MeOTAD are displayed in Figure 1. In the TA-St-CA structure, the diphenylaniline group is the electron donor, cyanoacrylic acid is the electron acceptor, and vinylene phenyl groups are the conjugate π bridge.[20] The single carboxyl group of the cyanoacrylic acid anchors the TA-St-CA structure to a Ti^{4+} site on the TiO_2 surface. In contrast, the Z907 dye adsorbs onto the TiO_2 surface *via* the two carboxyl groups on the bipyridine ligand. Figure 2 compares the absorption spectra of the TA-St-CA and Z907 dyes in an acetonitrile and *tert*-butyl alcohol solution; values of the maximum molar absorption coefficients are given in Table 1. The maximum molar absorption coefficient, ε_{max}, of the TA-St-CA dye in the visible region is 3.3×10^4 M^{-1} cm^{-1} at 411 nm, which is about 3 times larger than that of the Z907 dye ($\varepsilon_{max} = 0.99 \times 10^4$ M^{-1} cm^{-1}) at 530 nm.

The FE-SEM images in Figure 3a show a cross-sectional view of a SSDSSC consisting of a FTO layer covered with a porous, 3.2 μm thick 20 nm crystallite TiO_2 film. Spiro-MeOTAD fills the pores of the film and forms a 210 nm thick overlayer, which, in turn, is covered with a 190 nm thick layer of silver, which serves as an electrical contact. Figure 3b shows a cross-sectional view of spiro-MeOTAD-free, 20 nm crystallite TiO_2 film. Figure 3c shows a magnified view of a region of the TiO_2 film in Figure 3a. It can be seen that spiro-MeOTAD fills the pores of the film.

Figure 4a compares the $J-V$ characteristics of the solid-state dye-sensitized solar cell and the iodide electrolyte-based DSSC with the TA-St-CA and Z907 sensitizer under simulated AM1.5 solar light (100 mW/cm^2). The iodide electrolyte-based DSSC with TA-St-CA displayed a V_{oc} of 719 mV, which was 44 mV less than the V_{oc} (763 mV) of the DSSC with the ruthenium Z907 dye. On the other hand, the SSDSSC with the TA-St-CA sensitizer exhibited a V_{oc} of 1020 mV, which was 171 mV higher than the V_{oc} (849 mV) of the solid-state cell with the Z907 sensitizer. In both cases, the solid-state cells displayed higher open-circuit voltages than those of the liquid redox electrolyte-based DSSCs, irrespective of the choice of dye, for reasons discussed below. The short-circuit current densities (J_{sc}) of the iodide electrolyte-based DSSC with either the TA-St-CA or ruthenium Z907 sensitizer were the same, about 7.8 mA/cm^2. However, the J_{sc} of the solid-state cell with the TA-St-CA dye was 4.25 mA/cm^2, which was 2.2 mA/cm^2 lower than that of the iodide electrolyte-based DSSC with the Z907 dye. Figure 4b shows the IPCE spectra of the solid-state cell and liquid redox electrolyte-based DSSC with the TA-St-CA and Z907 sensitizer. In the spectral range between 350 and 510 nm, the iodide electrolyte-based DSSC exhibits significantly higher IPCE values with the TA-St-CA dye than with the Z907 dye. This is attributable at least, in part, to the molar absorption coefficients of TA-St-CA dye being about 3 times higher than those of the Z907 dye over this spectral range (Figure 2). In the spectral region at longer wavelengths (>510 nm), the iodide electrolyte-based DSSC shows larger IPCE values with the Z907 dye than with TA-St-CA dye. This observation is not surprising considering that the absorbance of TA-St-CA is close to zero at wavelengths longer than 600 nm (Figure 2). Taking into account the entire IPCE spectra, the similar J_{sc} values of the iodide electrolyte-based DSSCs with the TA-St-CA and Z907 sensitizers are understandable. Compared with the liquid electrolyte-based DSSC with the TA-St-CA dye, the IPCE response of the SSDSSC with the TA-St-CA dye is significantly reduced over the same spectral range (Figure 4b). In part, the difference is due to partial overlap of absorption spectra of the TA-St-CA dye and

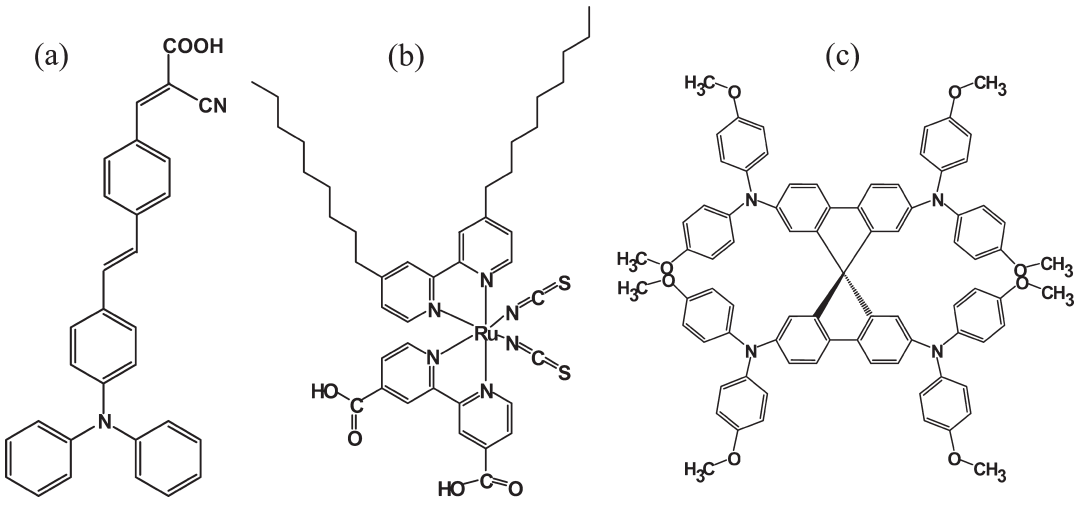

Figure 1. Structures of (a) TA-St-CA dye, (b) Z907 dye, and (c) spiro-MeOTAD.

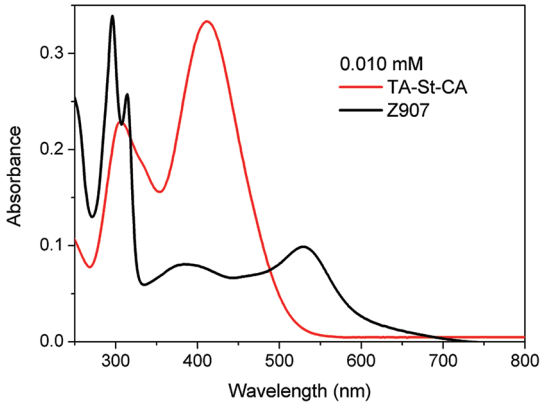

Figure 2. UV−vis absorbance spectra of TA-St-CA and Z907 dyes in *tert*-butyl alcohol/acetonitrile (1:1, v/v); the concentrations of the TA-St-CA and Z907 dyes were 1.0×10^{-5} M.

the spiro-MeOTAD. Spiro-MeOTAD has an absorption band between 330 and 410 nm with a maximum at about 389 nm ($\varepsilon_{max} = 7.47 \times 10^4$ M^{-1} cm^{-1}),[12] which is close to the absorption maximum of the TA-St-CA dye at 411 nm ($\varepsilon_{max} = 3.3 \times 10^4$ M^{-1} cm^{-1}; Table 1). Thus, spiro-MeOTAD attenuates some of the light before it reaches the TA-St-CA dye, leading to a loss of photocurrent density in the SSDSSC. For a similar reason, light absorption by spiro-MeOTAD also lowers the J_{sc} of the SSDSSC with the TA-St-CA dye compared with that of the iodide electrolyte-based DSSC with the Z907 dye. It is worth noting that the J_{sc} values calculated based on the IPCE and AM1.5 solar spectra were consistent (within ±10% error) with the J_{sc} values in Table 1. It is also noteworthy that there is a substantial difference between the absorption spectrum of TA-St-CA in a *tert*-butyl alcohol/acetonitrile solution (Figure 2) and the IPCE curves for the liquid electrolyte-based and solid-state cells with TA-St-CA (Figure 4b). This is due, in part, to the presence or absence of either the iodide

TABLE 1. Comparison of Molar Absorption Coefficients at Peak Maxima of TA-St-CA and Z907 in *tert*-Butyl Alcohol/Acetonitrile (1:1, v/v)

dye	λ_{max} (nm) (ε_{max} (10^4 M^{-1} cm^{-1}))
TA-St-CA	305 (2.29), 411 (3.33)
Z907	385 (0.81), 530 (0.99)

electrolyte or spiro-MEOTAD and the extent to which one of the latter attenuates the light before it reaches the TA-St-CA-covered films in the cells.

Figure 5 shows the effects of different sensitizers and hole-conducting phases (solid state *vs* liquid redox electrolyte) on the photoelectron densities (n_{oc}) in TiO_2 at different open-circuit voltages. Values of n_{oc} were determined using procedures described elsewhere.[21] The photoelectron densities at V_{oc} were calculated from the expression $n_{oc} = J_{sc}\tau_r/qd(1 - P)$, where τ_r is the recombination time constant (or electron lifetime) determined from intensity-modulated photovoltage spectroscopy (IMVS) measurements as a function of bias light intensity, q is the elementary charge, d is the film thickness, and P is the film porosity. The solid-type DSSCs with the TA-St-CA or Z907 sensitizer display the same n_{oc} dependence on V_{oc}. Similarly, the iodide electrolyte-based DSSCs with the TA-St-CA or Z907 dye showed no substantive difference in the V_{oc} dependence of the photoelectron density. However, when compared at the same n_{oc}, the open-circuit voltages of the solid-state cells were about 300−350 mV higher than those of the iodide electrolyte-based DSSCs. The open-circuit voltage of a DSSC is defined as the difference between the quasi-Fermi level of electrons in TiO_2 in the light and the Fermi level in the dark, which is the same as the Fermi level of the hole-conducting phase (liquid redox electrolyte or HTM).[22] Normally, at a constant photoelectron density, V_{oc} is fixed except in the case of band-edge movement.

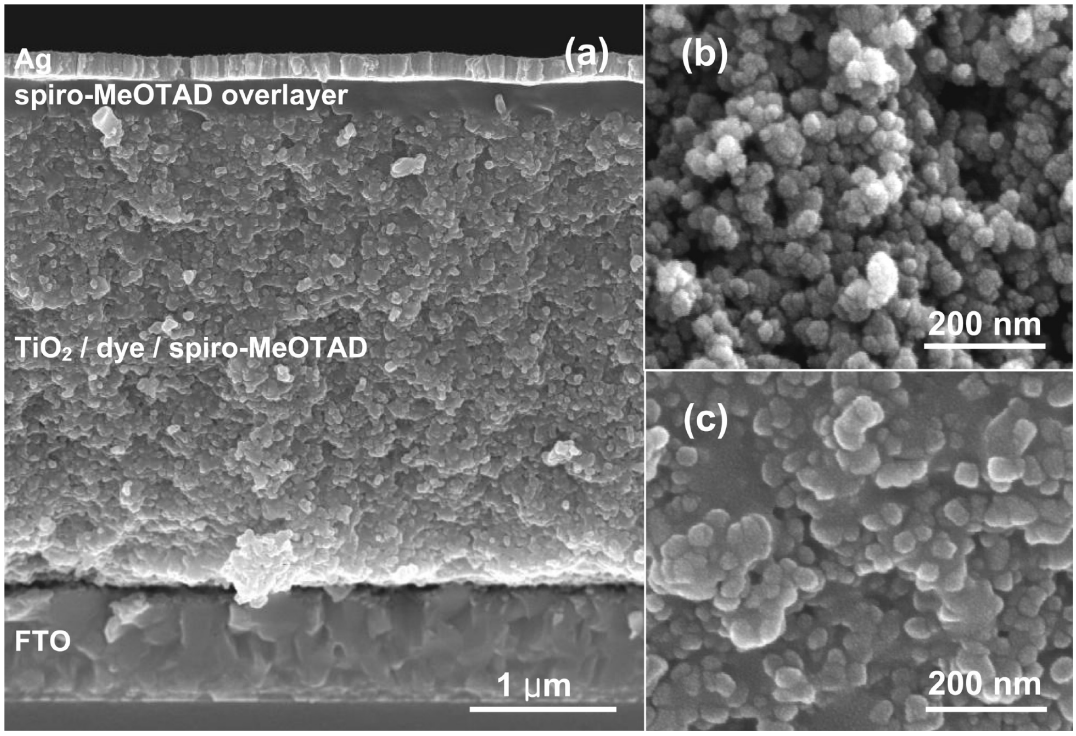

Figure 3. Cross-sectional view of FE-SEM images of (a) a SSDSSC consisting of a FTO layer, porous layer of titania nanocrystalline film filled with spiro-MeOTAD, spiro-MeOTAD overlayer, and silver layer, (b) spiro-MeOTAD-free TiO_2 film, and (c) spiro-MeOTAD-filled TiO_2 film.

Band-edge movement occurs when a sufficient net number of charges (or dipoles) build up on the surface of the particles to induce a change in the potential drop across the Helmholtz layer.[23] A net-negative surface charge buildup can cause the band edges to move upward, leading to a higher photovoltage.[23,24] A net-positive surface charge buildup can cause the band edges to move downward, resulting in a lower photovoltage.[25] For example, lower photovoltages result from adding adsorptive cations, such as Li^+, to the electrolyte, owing to a positive surface charge buildup causing the band edge to move downward, toward positive electrochemical potentials.[26] In the current study, the liquid electrolyte used in the DSSCs contained 0.2 M Li^+, whereas the spiro-MeOTAD used in the solid-state DSSCs contained 0.02 M lithium salt. Because of the lower Li^+ concentration used with spiro-MeOTAD, the conduction band edge of TiO_2 is expected to be at more negative potentials in solid-state DSSCs than in the liquid electrolyte-based cells. On the basis of the results of a recent study[27] on the effect of Li^+ concentration on charge-carrier dynamics in DSSCs, we estimate that decreasing the Li^+ concentration from 0.2 to 0.02 M results in an 80 mV negative potential shift of the TiO_2 conduction band edge in the solid-state DSSC, which is substantially smaller than the 300−350 mV lower V_{oc} that is evident in Figure 5. So, what other factor can significantly result in the differences in the open-circuit voltage? We attribute the difference to the redox potentials of the hole-conducting phases. The redox potential of the I_3^-/I^- couple in the liquid electrolyte is about 0.4 V (*vs* NHE), whereas the one-electron oxidation potential of spiro-MeOTAD$^+$/spiro-MeOTAD couple is about 0.82 V (*vs* NHE).[28] Therefore, the observed increase in V_{oc} at a fixed photoelectron density is ascribed mainly to high oxidation potential of the organic solid-state hole-transporting material spiro-MeOTAD compared with the redox potential of the I_3^-/I^- couple in the liquid electrolyte. This conclusion is in agreement with that of others.[17]

Figure 6 provides information on the effect of the sensitizers and hole-conducting media (spiro-MeOTAD and iodide electrolyte) on the capacitances (C_μ) at different applied voltages for the SSDSSC and liquid redox electrolyte DSSC. From the expression $C_\mu \propto \exp(qV/mkT)$, where k is the Boltzmann constant, T is the absolute temperature, and m is related to the shape of the distribution of the density of states, which can be determined from the slope of the capacitance *versus* voltage plot. Because plots have essentially the same slopes, the shape of the trap state distribution is the same, independent of the dye and hole-conducting phase. For the same capacitance, the voltages of the solid-state cells are about 350 mV higher than those of the liquid redox electrolyte-based DSSCs. This result is consistent with the conclusion drawn from the analysis of Figure 5 that the redox potentials of the iodide electrolyte and spiro-MeOTAD account for difference between V_{oc} of the solid-state DSSC and the liquid electrolyte-based DSSC at a fixed photoelectron

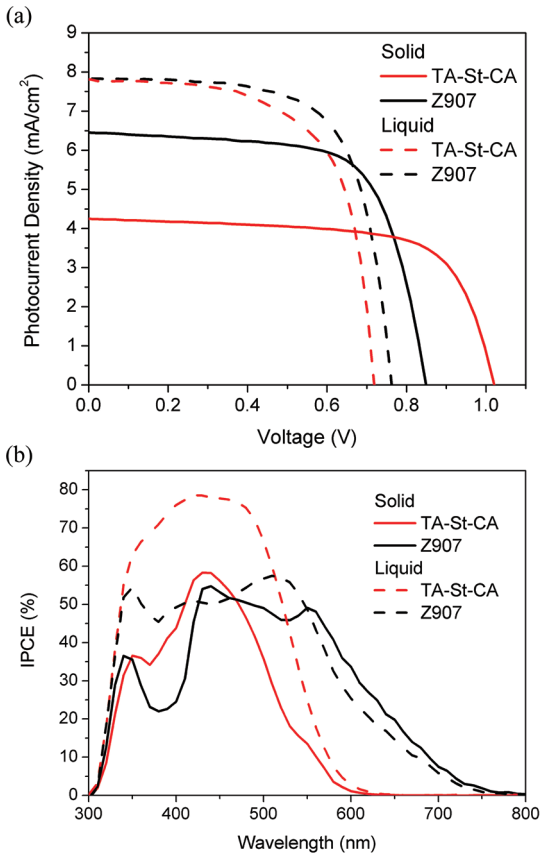

Figure 4. (a) $J-V$ characteristics and (b) IPCE spectra of a solid-state dye-sensitized solar cell and an iodide electrolyte-based DSSC with TA-St-CA and Z907 sensitizers; the TiO_2 films contain 20 nm sized crystallites and are 3.5 μm thick; simulated AM1.5 solar light (100 mW/cm^2).

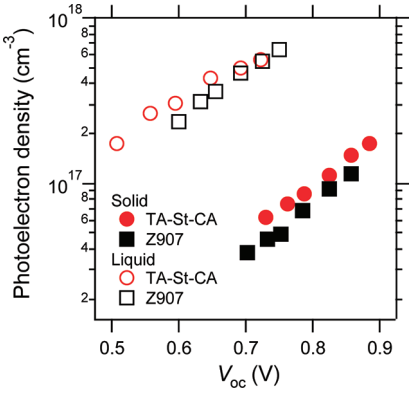

Figure 5. Relationship of the photoelectron density to the open-circuit voltage (V_{oc}) for solid-state and liquid electrolyte-based DSSCs with the TA-St-CA and Z907 dye.

density. Also, regardless of hole-conducting media, the Z907- and TA-St-CA-based DSSCs display approximately the same capacitance dependence on the voltage across the entire voltage range. This suggests that the extent of band-edge movement (if any) induced by TA-St-CA and Z907 is the same.

Figure 7 shows the effect of the sensitizers and hole-conducting phases on the recombination time

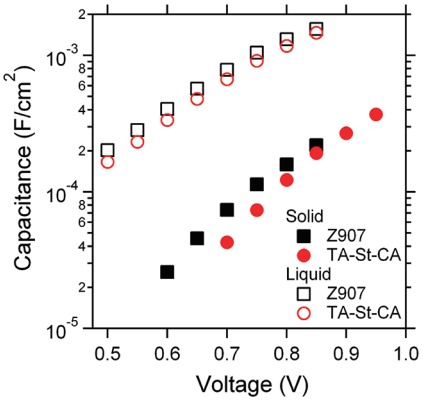

Figure 6. Dependence of the capacitance on the applied voltage for solid-state and liquid electrolyte-based DSSCs with the TA-St-CA and Z907 dye.

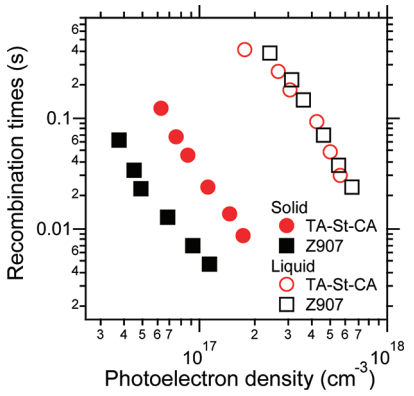

Figure 7. Dependence of the recombination times on the photoelectron density for solid-state and liquid electrolyte-based DSSCs with the TA-St-CA and Z907 dye.

constants (τ_r) at different photoelectron densities at open circuit. Independent of the choice of sensitizer, the recombination times at a fixed n_{oc} are much longer for the liquid electrolyte-based DSSCs than for the solid-state DSSCs, implying that the interfacial electron transfer from TiO_2 to the oxidized spiro-MeOTAD is faster in solid-state DSSCs. This observation is in agreement with another study.[13] Moreover, the recombination times for iodide electrolyte-based cells with TA-St-CA and Z907 dyes are the same. In marked contrast, recombination is 6 times slower in the solid-state DSSCs with the TA-St-CA dye than with the Z907 dyes under the same condition of constant n_{oc}. Differences in the recombination kinetics are attributed to steric hindrance associated with the TA-St-CA and Z907 adsorption geometries and the accessibility of I_3^- in the iodide electrolyte and spiro-MeOTAD$^+$ in the hole-transfer material to the TiO_2 surface. In iodide electrolyte-based cells, the small size of I_3^- (<1 nm)[29] enables it to approach the TiO_2 surface closely, irrespective of the selected sensitizer. However, for the solid-state DSSCs, the adsorption geometry of the TA-St-CA and Z907 dye and the size of oxidized spiro-MeOTAD (2 nm)[12] can affect the distance of closest approach

to the TiO_2 surface. The closest spiro-MeOTAD$^+$ can approach the TiO_2 surface is about 2 nm, corresponding to the distance between the anchoring group on the TiO_2 surface and the donor group of the TA-St-CA dye as calculated using the density functional theory with Gaussian03 package. For comparison, the size of the Z907 dye is $\ll$2 nm.[30] Consequently, one would expect, as is observed for the SSDSSC, that the TA-St-CA dye is more effective than the Z907 dye in suppressing recombination at the TiO_2/spiro-MeOTAD interface. In addition to steric hindrance, recombination of electrons from TiO_2 to the oxidized TA-St-CA sensitizer may be slower than from TiO_2 to the oxidized Z907 dye in the solid-state cell. In the liquid electrolyte-based DSSC, the back electron transfer from TiO_2 to the oxidized dye is less important because of the very rapid regeneration of the dye by iodide ions in solution following electron injection. Considering the difference in recombination times and short-circuit photocurrent densities (Table 2) for the solid-state DSSCs, we estimated from the expression $n_{oc} \propto J_{sc}\tau_r$ that the photoelectron density with the TA-St-CA sensitizer is about a factor 4 larger than that with the Z907 sensitizer. Furthermore, from the analysis of the n_{oc} *versus* V_{oc} plots for SSDSSCs (Figure 5), we estimate that the 4-fold increase of n_{oc} would lead to about a 180 mV higher V_{oc}, which agrees with the observed 171 mV change in V_{oc} (Table 2). These results imply that the TA-St-CA dye enhances the voltages of the solid-state DSSC by retarding recombination. However, as discussed above, there is no evidence that the TA-St-CA dye contributes to the voltage by inducing band-edge movement (Figure 5). The voltage-enhancement mechanism of the solid-state DSSC sensitized with TA-St-CA dye differs from the mechanism invoked involving a similar type of solid-state cell sensitized with a different organic dye.[17] The high V_{oc} obtained with the latter cell was attributed to the organic dye shifting the TiO_2 conduction band edge toward more negative electrode potentials; the dye had no effect, however, on the recombination kinetics. Thus, while both solid-state cells with organic dyes produced comparably high open-circuit voltages, the voltage-enhancement mechanism of the two organic dyes differed significantly.

TABLE 2. *J*–*V* Characteristics of SSDSSC and Iodide Electrolyte-Based DSSCs with the TA-St-CA and Z907 Sensitizers under Simulated AM1.5 Light

cell	sensitizer	V_{oc} (mV)	J_{sc} (mA/cm^2)	FF (%)	η (%)	film thickness (μm)
solid state	TA-St-CA	1020	4.25	68.9	3.0	3.5
	Z907	849	6.45	68.3	3.7	
liquid	TA-St-CA	719	7.81	64.2	3.6	3.3
	Z907	763	7.83	67.7	4.0	

CONCLUSIONS

Sensitization of solid-state dye-sensitized solar cells (SSDSSCs) with a newly developed organic dye, TA-St-CA, with a high molar absorption coefficient leads to a high open-circuit voltage. Investigation of the voltage-enhancement mechanism revealed that the TA-St-CA dye contributes to the high voltage *via* its reduction of the loss of photoelectron density resulting from recombination. Theoretical modeling suggests that the TA-St-CA dye shields the electrons in the TiO_2 film from reacting with spiro-MeOTAD$^+$. While the organic dye retarded recombination, it did not contribute to the voltage by inducing band-edge movement, which contrasts with the situation for a different organic dye. The latter dye is reported to shift the band edges to negative potentials but had no effect on recombination. Thus, although SSDSSCs with either organic dye produced comparably high voltages, the voltage-enhancement mechanism of the two sensitizers differed substantially. Designing dyes with the capacity to suppress recombination and shift the band edges to more negative potentials concomitantly could lead to still higher voltages. Besides developing organic sensitizers with strong absorption and sensitizing properties, this study provides insight into other properties of a dye that could further enhance the cell voltage.

METHODS

Fluorine-doped transparent conducting SnO_2 (FTO) glass plates (Pilkington, 2.3 mm thick, 8 Ω/sq) were laser-etched and then cleaned with distilled water and ethanol. After drying the plates in air, they were subjected to UV/ozone plasma for 20 min to remove organic residues. A thin compact layer of titanium oxide was deposited on the cleaned FTO plates by spin coating a solution of 0.15 M titanium diisopropoxide bis(acetylacetonate) in 1-butanol and then spinning two more times a 0.3 M solution of the same titanium complex; the resulting deposit was heated at 125 °C for 5 min after each spin coating. To control the TiO_2 film thickness, 0.5 cm width of the FTO plate was covered along the length of two edges with adhesive tape, having a nominal thickness of 37 μm. Pastes of either 20 or 35 nm TiO_2 crystallites were deposited on the FTO surface. For a majority of the studies, the TiO_2 films contained 20 nm sized crystallites. For the electron dynamic studies, films of 35 nm sized TiO_2 particles were used. The TiO_2 nanoparticles were synthesized as described elsewhere.[31−33] After removing the adhesive tapes, the assemblage was heated in air at 500 °C for 30 min and then allowed to cool. The final film thicknesses were about 2−3 μm as determined with a surface profiler and confirmed using FE-SEM. The respective porosity and the specific surface of the films were about 60% and 65 m^2/g. The films were then soaked in 0.02 M $TiCl_4$ solution at room temperature for 12 h and then rinsed with distilled water. After heating the films again at 500 °C in air for 30 min and then cooling them to 80 °C, they were immersed for 4 h in *tert*-butyl alcohol/acetonitrile (1:1, v/v) at 50 °C containing either 0.3 mM Ru(4,4′-dicarboxylic acid-2,2′-bipyridine)(4,4′-dinonyl-2,2′-bipyridine)(NCS)$_2$ (Z907) or 0.3 mM (*E*)-2-cyano-3-(4-(4-(diphenlyamino)styryl)phenyl)acrylic acid (TA-St-CA). TA-St-CA was synthesized by procedures described

in the literature.[7] Semitransparent counter electrodes for the liquid redox electrolyte-based DSSCs were prepared by spreading a droplet of 7 mM H_2PtCl_6 in 2-propanol onto the FTO plates (Pilkington, 2.3 mm thickness, 15 Ω/sq) and subsequently heating them at 400 °C for 20 min. The Pt-covered counter electrode was placed over the TiO_2 electrode, and the assemblage was sealed with 1.0 mm wide strips of a 25 μm thick Surlyn (Dupont grade 1702). The redox electrolyte consisted of 0.7 M 1-propyl-3-methyl imidiazolium iodide (PMII), 0.05 M iodine (I_2), 0.2 M LiI, and 0.5 M *tert*-butylpyridine in acetonitrile/3-methoxypropionitrile (1:1, v/v). The HTM was prepared from a mixture of 0.14 M spiro-MeOTAD in chlorobenzene, 21 mM bis(trifluoromethane-)sulfonimide lithium in acetonitrile, and 0.11 M *tert*-butylpyridine. The spiro-MeOTAD solution was deposited onto the dye-covered TiO_2 film and allowed to diffuse into the pores of the TiO_2 film for 1.5 min prior to spin coating the film at 2000 rpm for 30 s in air. Next, a 200 nm thick Ag contact was thermally evaporated onto the films through a shadow mask to complete the cell.

Photocurrent−voltage (*J*−*V*) measurements were performed using a Keithley 2400 source measure unit. The irradiation source was an ozone-free 1000 W xenon light source (Oriel 91193), and its light intensity was adjusted for 1 sun light intensity (100 mW/cm^2) using an NREL-calibrated Si solar cell equipped with a KG-5 filter for approximating AM1.5 solar irradiance. The incident photon-to-current conversion efficiency (IPCE) as a function of excitation wavelength was obtained with an IPCE measurement system (PV Measurements, Inc.). UV−visible absorbance spectra of the dyes were measured with a UV−visible spectrophotometer (Agilent 8453). The thickness of TiO_2 films was obtained by using an Alpha-Step IQ surface profiler (KLA Tencor). The thicknesses of the HTM overlayer were determined using field emission scanning electron microscopy (FE-SEM; Hitachi S4100). Transport and recombination time constants were measured by intensity-modulated photocurrent spectroscopy (IMPS) and IMVS as described previously.[23,34] For these measurements, the cells were probed with a modulated beam of 680 nm light superimposed on a relatively large background (bias) illumination also at 680 nm. The probe and bias light entered the cell from the working electrode side. Electrochemical impedance (EIS) was used to determine the capacitance of the cells as detailed elsewhere.[34] The EIS measurements were performed with a potentiostat/frequency analyzer (PARSTAT 2273) using a two-electrode configuration. The modulation frequencies range from 50 mHz to 100 kHz. The amplitude of the modulation voltage was 10 mV.

Acknowledgment. This work was supported by the Division of Chemical Sciences, Geosciences, and Biosciences, Office of Basic Energy Sciences (A.J.F.) and the Division of Photovoltaics, Office of Utility Technologies, (K.Z., S.-R.J.), U.S. Department of Energy, under Contract No. DEAC36-08GO28308. This work was also supported by the National Research Foundation of Korea grant funded by the Ministry of Education, Science and Technology of Korea under Contract No. 2011-0016441 and the Korea Institute of Energy Technology Evaluation and Planning grant funded by the Ministry of Knowledge Economy under Contract No. 20103020010010 (N.-G.P.), and the Korea Institute of Science and Technology internal research fund (K.K.).

REFERENCES AND NOTES

1. O'Regan, B.; Grätzel, M. A Low-Cost, High-Efficiency Solar-Cell Based on Dye-Sensitized Colloidal TiO_2 Films. *Nature* **1991**, *353*, 737–740.
2. Chiba, Y.; Islam, A.; Watanabe, Y.; Komiya, R.; Koide, N.; Han, L. Y. Dye-Sensitized Solar Cells with Conversion Efficiency of 11.1%. *Jpn. J. Appl. Phys.* **2006**, *45*, L638–L640.
3. Nazeeruddin, M. K.; De Angelis, F.; Fantacci, S.; Selloni, A.; Viscardi, G.; Liska, P.; Ito, S.; Bessho, T.; Grätzel, M. Combined Experimental and DFT-TDDFT Computational Study of Photoelectrochemical Cell Ruthenium Sensitizers. *J. Am. Chem. Soc.* **2005**, *127*, 16835–16847.
4. Choi, H.; Baik, C.; Kang, S. O.; Ko, J.; Kang, M. S.; Nazeeruddin, M. K.; Grätzel, M. Highly Efficient and Thermally Stable Organic Sensitizers for Solvent-Free Dye-Sensitized Solar Cells. *Angew. Chem., Int. Ed.* **2008**, *47*, 327–330.
5. Wang, Z. S.; Koumura, N.; Cui, Y.; Takahashi, M.; Sekiguchi, H.; Mori, A.; Kubo, T.; Furube, A.; Hara, K. Hexylthiophene-Functionalized Carbazole Dyes for Efficient Molecular Photovoltaics: Tuning of Solar-Cell Performance by Structural Modification. *Chem. Mater.* **2008**, *20*, 3993–4003.
6. Zhang, G. L.; Bala, H.; Cheng, Y. M.; Shi, D.; Lv, X. J.; Yu, Q. J.; Wang, P. High Efficiency and Stable Dye-Sensitized Solar Cells with an Organic Chromophore Featuring a Binary π-Conjugated Spacer. *Chem. Commun.* **2009**, 2198–2200.
7. Hwang, S.; Lee, J. H.; Park, C.; Lee, H.; Kim, C.; Lee, M. H.; Lee, W.; Park, J.; Kim, K.; Park, N. G. A Highly Efficient Organic Sensitizer for Dye-Sensitized Solar Cells. *Chem. Commun.* **2007**, 4887–4889.
8. Bach, U.; Lupo, D.; Comte, P.; Moser, J. E.; Weissortel, F.; Salbeck, J.; Spreitzer, H.; Grätzel, M. Solid-State Dye-Sensitized Mesoporous TiO_2 Solar Cells with High Photon-to-Electron Conversion Efficiencies. *Nature* **1998**, *395*, 583–585.
9. Snaith, H. J.; Schmidt-Mende, L. Advances in Liquid-Electrolyte and Solid-State Dye-Sensitized Solar Cells. *Adv. Mater.* **2007**, *19*, 3187–3200.
10. Bach, U.; Tachibana, Y.; Moser, J. E.; Haque, S. A.; Durrant, J. R.; Grätzel, M.; Klug, D. R. Charge Separation in Solid-State Dye-Sensitized Heterojunction Solar Cells. *J. Am. Chem. Soc.* **1999**, *121*, 7445–7446.
11. Kruger, J.; Plass, R.; Cevey, L.; Piccirelli, M.; Grätzel, M.; Bach, U. High Efficiency Solid-State Photovoltaic Device Due to Inhibition of Interface Charge Recombination. *Appl. Phys. Lett.* **2001**, *79*, 2085–2087.
12. Ding, I. K.; Tetreault, N.; Brillet, J.; Hardin, B. E.; Smith, E. H.; Rosenthal, S. J.; Sauvage, F.; Grätzel, M.; McGehee, M. D. Pore-Filling of Spiro-OMeTAD in Solid-State Dye Sensitized Solar Cells: Quantification, Mechanism, and Consequences for Device Performance. *Adv. Funct. Mater.* **2009**, *19*, 2431–2436.
13. Fabregat-Santiago, F.; Bisquert, J.; Cevey, L.; Chen, P.; Wang, M. K.; Zakeeruddin, S. M.; Grätzel, M. Electron Transport and Recombination in Solid-State Dye Solar Cell with Spiro-OMeTAD as Hole Conductor. *J. Am. Chem. Soc.* **2009**, *131*, 558–562.
14. Schmidt-Mende, L.; Zakeeruddin, S. M.; Grätzel, M. Efficiency Improvement in Solid-State-Dye-Sensitized Photovoltaics with an Amphiphilic Ruthenium-Dye. *Appl. Phys. Lett.* **2005**, *86*, 13504.
15. Schmidt-Mende, L.; Grätzel, M. TiO_2 Pore-Filling and Its Effect on the Efficiency of Solid-State Dye-Sensitized Solar Cells. *Thin Solid Films* **2006**, *500*, 296–301.
16. Snaith, H. J.; Humphry-Baker, R.; Chen, P.; Cesar, I.; Zakeeruddin, S. M.; Grätzel, M. Charge Collection and Pore Filling in Solid-State Dye-Sensitized Solar Cells. *Nanotechnology* **2008**, *19*, 424003.
17. Chen, P.; Yum, J. H.; De Angelis, F.; Mosconi, E.; Fantacci, S.; Moon, S. J.; Baker, R. H.; Ko, J.; Nazeeruddin, M. K.; Grätzel, M. High Open-Circuit Voltage Solid-State Dye-Sensitized Solar Cells with Organic Dye. *Nano Lett.* **2009**, *9*, 2487–2492.
18. Lagref, J. J.; Nazeeruddin, M. K.; Grätzel, M. Molecular Engineering on Semiconductor Surfaces: Design, Synthesis and Application of New Efficient Amphiphilic Ruthenium Photo Sensitizers for Nanocrystalline TiO_2 Solar Cells. *Synth. Met.* **2003**, *138*, 333–339.
19. Kroeze, J. E.; Hirata, N.; Koops, S.; Nazeeruddin, M. K.; Schmidt-Mende, L.; Grätzel, M.; Durrant, J. R. Alkyl Chain Barriers for Kinetic Optimization in Dye-Sensitized Solar Cells. *J. Am. Chem. Soc.* **2006**, *128*, 16376–16383.
20. Zhang, C. R.; Liu, Z. J.; Chen, Y. H.; Chen, H. S.; Wu, Y. Z.; Feng, W. J.; Wang, D. B. DFT and TD-DFT Study on Structure and Properties of Organic Dye Sensitizer TA-St-CA. *Curr. Appl. Phys.* **2010**, *10*, 77–83.
21. Zhu, K.; Kopidakis, N.; Neale, N. R.; van de Lagemaat, J.; Frank, A. J. Influence of Surface Area on Charge Transport and Recombination in Dye-Sensitized TiO_2 Solar Cells. *J. Phys. Chem. B* **2006**, *110*, 25174–25180.
22. Frank, A. J.; Kopidakis, N.; van de Lagemaat, J. Electrons in Nanostructured TiO_2 Solar Cells: Transport, Recombination

and Photovoltaic Properties. *Coord. Chem. Rev.* **2004**, *248*, 1165–1179.
23. Schlichthorl, G.; Huang, S. Y.; Sprague, J.; Frank, A. J. Band Edge Movement and Recombination Kinetics in Dye-Sensitized Nanocrystalline TiO_2 Solar Cells: A Study by Intensity Modulated Photovoltage Spectroscopy. *J. Phys. Chem. B* **1997**, *101*, 8141–8155.
24. Neale, N. R.; Kopidakis, N.; van de Lagemaat, J.; Gratzel, M.; Frank, A. J. Effect of a Coadsorbent on the Performance of Dye-Sensitized TiO_2 Solar Cells: Shielding *versus* Band-Edge Movement. *J. Phys. Chem. B* **2005**, *109*, 23183–23189.
25. Kopidakis, N.; Neale, N. R.; Frank, A. J. Effect of An Adsorbent on Recombination and Band-Edge Movement in Dye-Sensitized TiO_2 Solar Cells: Evidence for Surface Passivation. *J. Phys. Chem. B* **2006**, *110*, 12485–12489.
26. Pelet, S.; Moser, J. E.; Grätzel, M. Cooperative Effect of Adsorbed Cations and Iodide on the Interception of Back Electron Transfer in the Dye Sensitization of Nanocrystalline TiO_2. *J. Phys. Chem. B* **2000**, *104*, 1791–1795.
27. Jennings, J. R.; Wang, Q. Influence of Lithium Ion Concentration on Electron Injection, Transport, and Recombination in Dye-Sensitized Solar Cells. *J. Phys. Chem. C* **2010**, *114*, 1715–1724.
28. Bach, U. Solid-State Dye-Sensitized Mesoporous TiO_2 Solar Cells. Ph.D. Dissertation, École Polytechnique Fédérale de Lausanne, Lausanne, Switzerland, 2000.
29. Said, F. F.; Bazinet, P.; Ong, T. G.; Yap, G. P. A.; Richeson, D. S. Hydrogen Bonding Motifs of *N*,*N*′,*N*″-Trisubstituted Guanidinium Cations with Spherical and Rodlike Monoanions: Syntheses and Structures of I^-, I_3^-, and SCN^- Salts. *Cryst. Growth Des.* **2006**, *6*, 258–266.
30. Fillinger, A.; Parkinson, B. A. The Adsorption Behavior of a Rutheninm-Based Sensitizing Dye to Nanocrystalline TiO_2—Coverage Effects on the External and Internal Sensitization Quantum Yields. *J. Electrochem. Soc.* **1999**, *146*, 4559–4564.
31. Neale, N. R.; Frank, A. J. Size and Shape Control of Nanocrystallites in Mesoporous TiO_2 Films. *J. Mater. Chem.* **2007**, *17*, 3216–3221.
32. Ito, S.; Murakami, T. N.; Comte, P.; Liska, P.; Gratzel, C.; Nazeeruddin, M. K.; Grätzel, M. Fabrication of Thin Film Dye Sensitized Solar Cells with Solar to Electric Power Conversion Efficiency Over 10%. *Thin Solid Films* **2008**, *516*, 4613–4619.
33. Koo, H. J.; Park, J.; Yoo, B.; Yoo, K.; Kim, K.; Park, N. G. Size-Dependent Scattering Efficiency in Dye-Sensitized Solar Cell. *Inorg. Chim. Acta* **2008**, *361*, 677–683.
34. van de Lagemaat, J.; Park, N. G.; Frank, A. J. Influence of Electrical Potential Distribution, Charge Transport, and Recombination on the Photopotential and Photocurrent Conversion Efficiency of Dye-Sensitized Nanocrystalline TiO_2 Solar Cells: A Study by Electrical Impedance and Optical Modulation Techniques. *J. Phys. Chem. B* **2000**, *104*, 2044–2052.